Supporting Information

Liquid phase reduction synthesis of cobalt boride-activated carbon composite with improved specific capacitance and retention rate as a new positive electrode material for supercapacitors

Jing-Feng Hou [a], Jian-Fei Gao [a], Ling-Bin Kong [a, b,*]

[a] State Key Laboratory of Advanced Processing and Recycling of Non-Ferrous Metals, Lanzhou University of Technology, Lanzhou 730050, P. R. China

[b] School of Materials Science and Engineering, Lanzhou University of Technology, Lanzhou 730050, P. R. China

* Corresponding author. Tel.: +86 (0)931 2976579; Fax: +86 (0)931 2976578; E-mail: konglb@lut.cn

1. Experimental

1.1. Chemicals and materials

All chemicals in this work were analytical and can be used directly without purification. Cobalt chloride hexahydrate($CoCl_2·6H_2O$, >99%), sodium borohydride($NaBH_4$, >99%), sodium hydroxide(NaOH) and absolute ethanol (C_2H_5OH), were supplied by Sinopharm Chemical Reagent Co. Ltd(Shanghai, China). The experiment used deionized water with a resistivity of > 10.0 MΩ.

1.2. Synthesis of cobalt boride-activated carbon

In a typical experiment, cobalt boride nanoparticles were synthesized by liquid-phase synthesis method[1, 2]. 4 mmol $CoCl_2·6H_2O$ was added into 50 mL deionized water, which had been removed the dissolved oxygen by purging N_2. A certain amount of activated carbon was thrown into the solution, and the solution was kept on stirring for about half an hour. Dissolve 10 mmol $NaBH_4$ and 3 mmol NaOH in 20 mL deionized water. Then the aqueous solution of

$NaBH_4$ was dropwise added to cobalt chloride solution under continuous stirring. Severe frothing occurs if the sodium borohydride was added rapidly. After stirring for an hour, the obtained products were collected by suction filtration and washing which used distilled water and absolute ethanol. The black powder obtained after cleaning was dried at 60 °C for 12 h in a vacuum oven. Five dissimilar CoB-AC electrodes(C1, C2, C3, C4, C5) have been composed by adding different amounts of activated carbon(0.0096 g, 0.0191 g, 0.02871 g, 0.0383 g, 0.0479 g). The unsupported CoB(C0) was prepared by the same method with no activated carbon into the reactant solution.

1.3. Material characterization

The obtained C0, C3 were characterized by X-ray diffraction(XRD, Rigaku, D/MAX-2400) with a standard Cu Kα radiation source. Transmission electron microscope(TEM, JEOL JEM-2010) monitored The microstructure of samples. Nitrogen adsorption and desorption detection were achieved at 77 K using a surface area and pore size analyzer(JW-BK200). The specific surface areas of the samples were calculated by the Brumauer–Emmett–Teller(BET) theory. The mesopore and micropore size distribution was estimated from Barrett–Joyner–Halanda(BJH) method and Horvath–Kawazoe(HK) method, respectively.

1.4. Electrode preparation

The electrochemical behaviors of the CoB-AC composite electrodes were studied with a standard two-electrode system and a three-electrode device in a 6 M KOH alkaline aqueous electrolyte, in which Hg/HgO electrode and Pt sheet were used as the reference and counter electrodes, respectively. The working electrodes were made as follows[3]. The active material (C0, C1, C2, C3, C4, C5), acetylene black, and conducting graphite were mixed in a mass ratio of 80:7.5:7.5. Put them with polytetrafluoroethylene(PTFE, 5 wt%) binder and a few drops of ethanol onto a piece of foam nickel substrate(1 cm × 1 cm). Then dried at 60 °C for 12 h. The mass loading of nickel foam was 4 mg cm^2.

1.5. Electrochemical evaluation

The electrochemical capacitive performance was measured with a CHI660E tester(Shanghai, China). cyclic voltammetry(CV), galvanostatic charge-discharge(GCD) measurement and electrochemical impedance spectroscopy(EIS) measurement were employed to investigate electrochemical behaviors. The cycling performance was estimated using an electrochemical working station(CT2001A, Wuhan, China).

The specific capacitance(C, F g^{-1}) of the electrode materials can be calculated from the galvanostatic discharged curves according to the following eqn (1)[4]:

$$C=\frac{I\Delta t}{Vm} \quad \text{.....(1)}$$

where I is the current (mA), V is the potential (V), t is the discharge time (s), and m is the mass of the active material in the electrode (mg).

An asymmetric supercapacitor(ASC) configuration was constructed by using CoB-AC and AC as positive and negative electrodes face to face in 6 M KOH. The Q of each electrode depends on the specific capacitance(Cs), the potential range of the charge-discharge tests(V) and the mass of the active material(m) according to eqn (2)[4]:

$$Q=Cs\times V\times m \quad \text{.....(2)}$$

According to the charge-balance principle(Q+=Q-), where Q+ and Q- represent the charges stored in the positive and negative electrodes, respectively, the specific mass ratio of CoB-AC to AC was thus designed as 1.187:1 in such an asymmetric device. And the total mass of electroactive materials in the device is 4.478 mg. The calculation of specific capacitance(C_{device}), energy density(E), and power density(P) is based on the total mass of the cathode and anode according to eqn (3)–(5)[4]:

$$C_{device} = \frac{I\Delta t}{Vm} \quad \text{.....(3)}$$

$$E = \frac{1}{2} \times C_{device} \times V^2 \quad \text{.....(4)}$$

$$P = \frac{E}{t} \quad \text{.....(5)}$$

2. Supplementary results

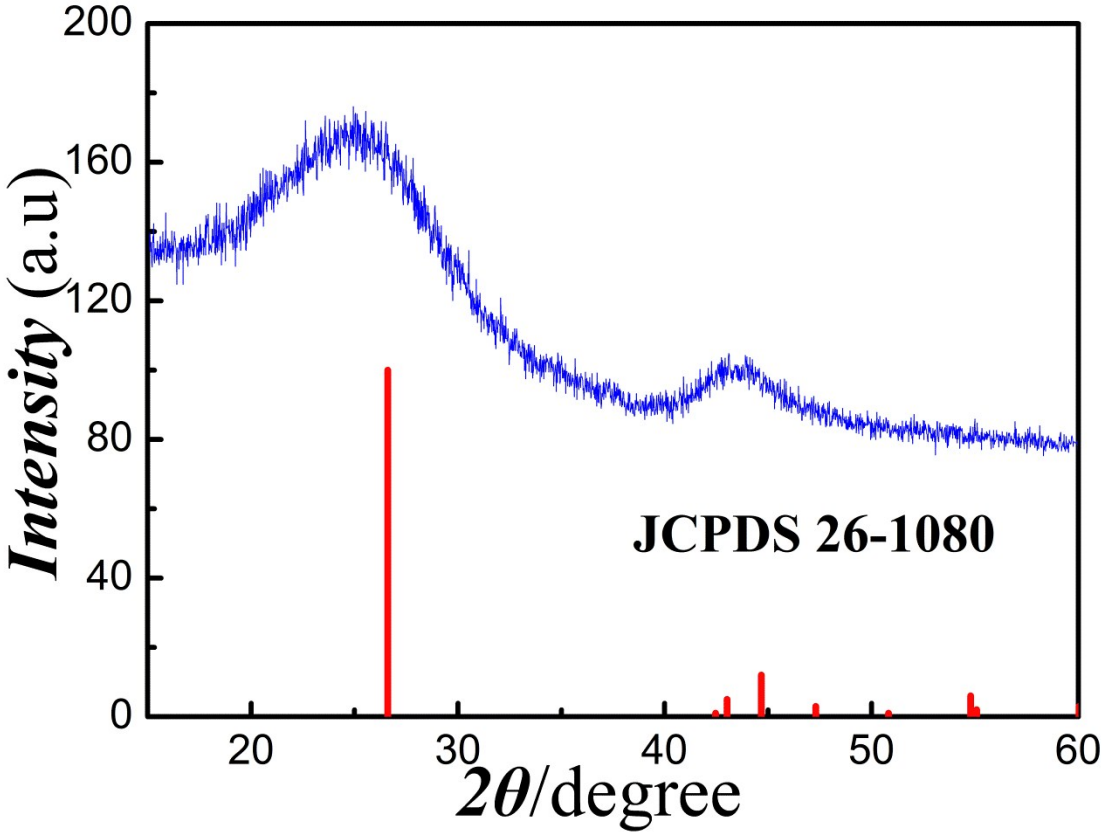

Figure S1. XRD pattern of activated carbon.

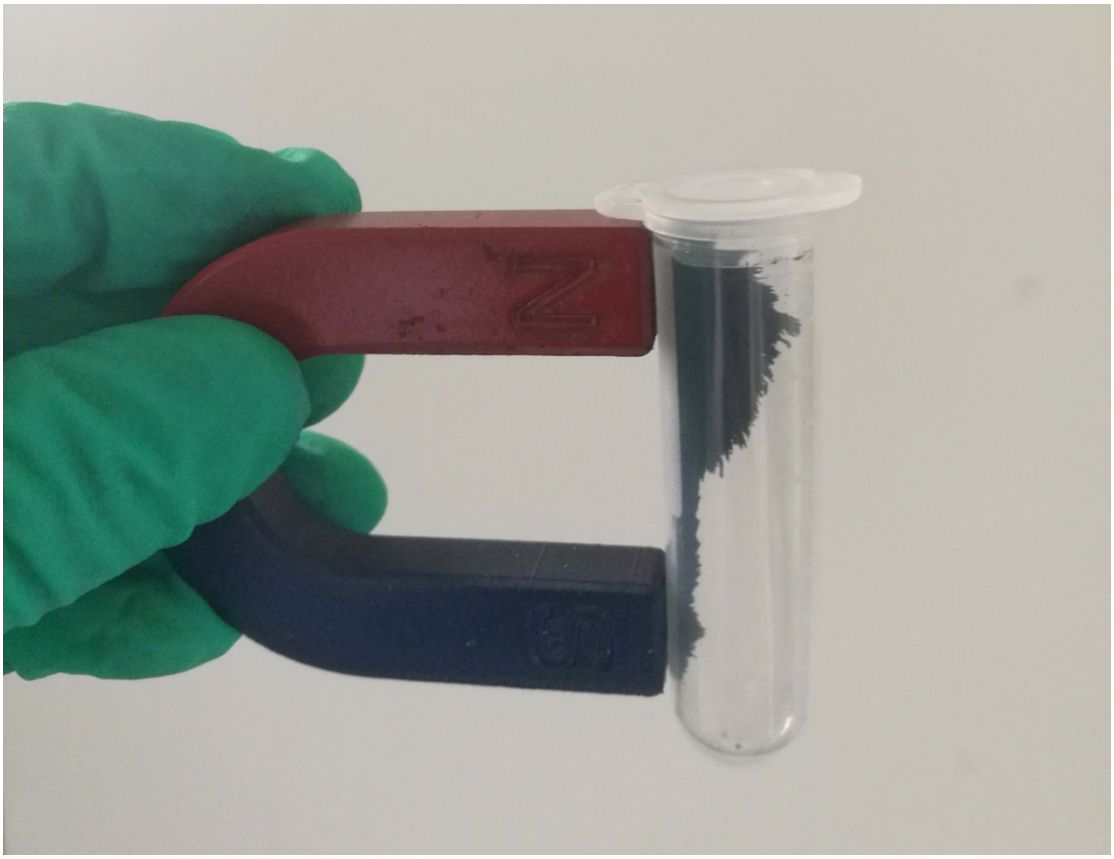

Figure S2. A photo of a sample of cobalt boride attracted by a U-shaped magnet showing the magnetic properties of the synthesized cobalt boride.

Sample	CoB wt%	C wt%
C0	100	0
C1	96.56	3.44
C2	93.35	6.65
C3	90.55	9.45
C4	87.86	12.14
C5	85.04	14.96

Table S1. Material composition (wt %) of the CoB-AC samples.

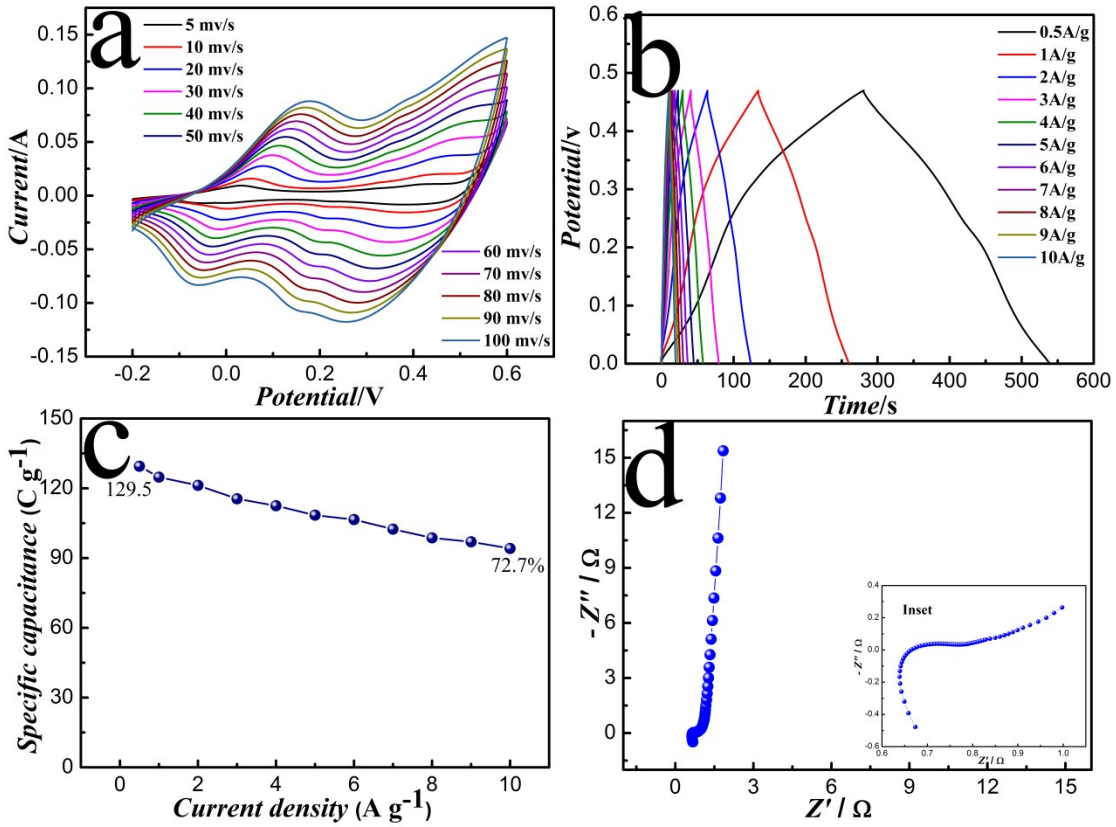

Figure S3. Three-electrode electrochemical measurements of the CoB-AC-0(C0) electrode.

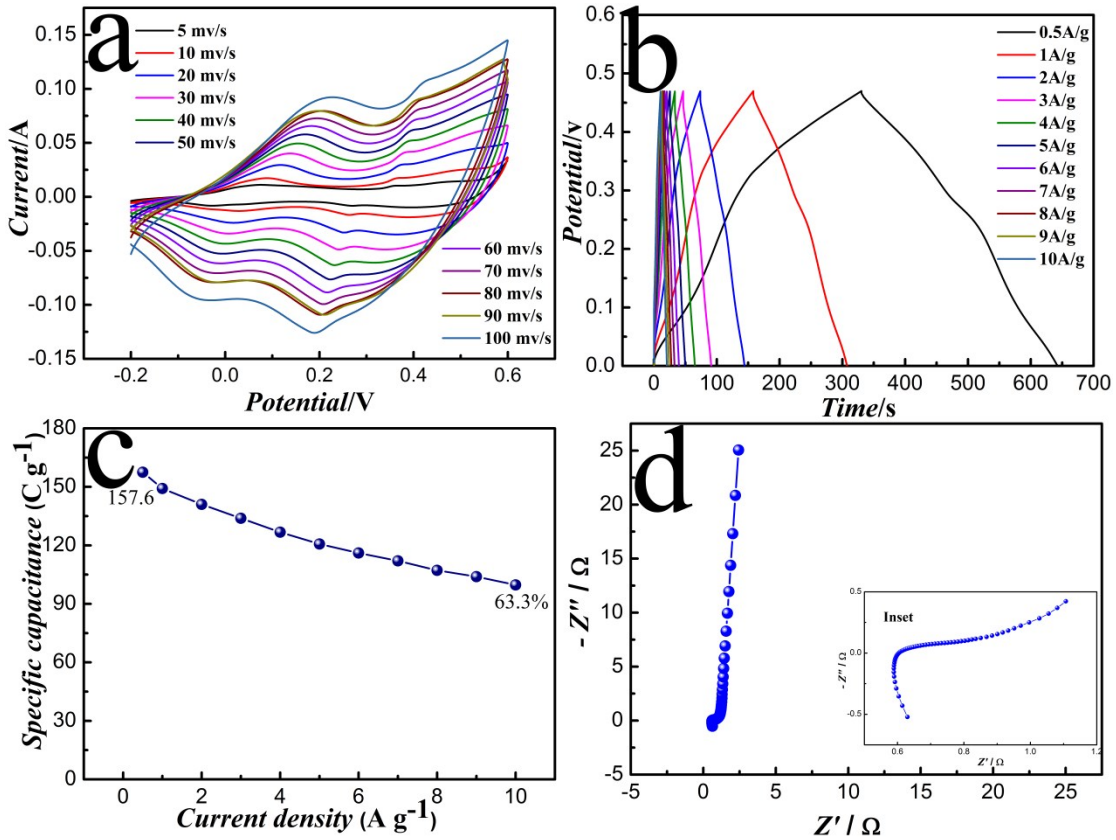

Figure S4. Three-electrode electrochemical measurements of the CoB-AC-1(C1) electrode.

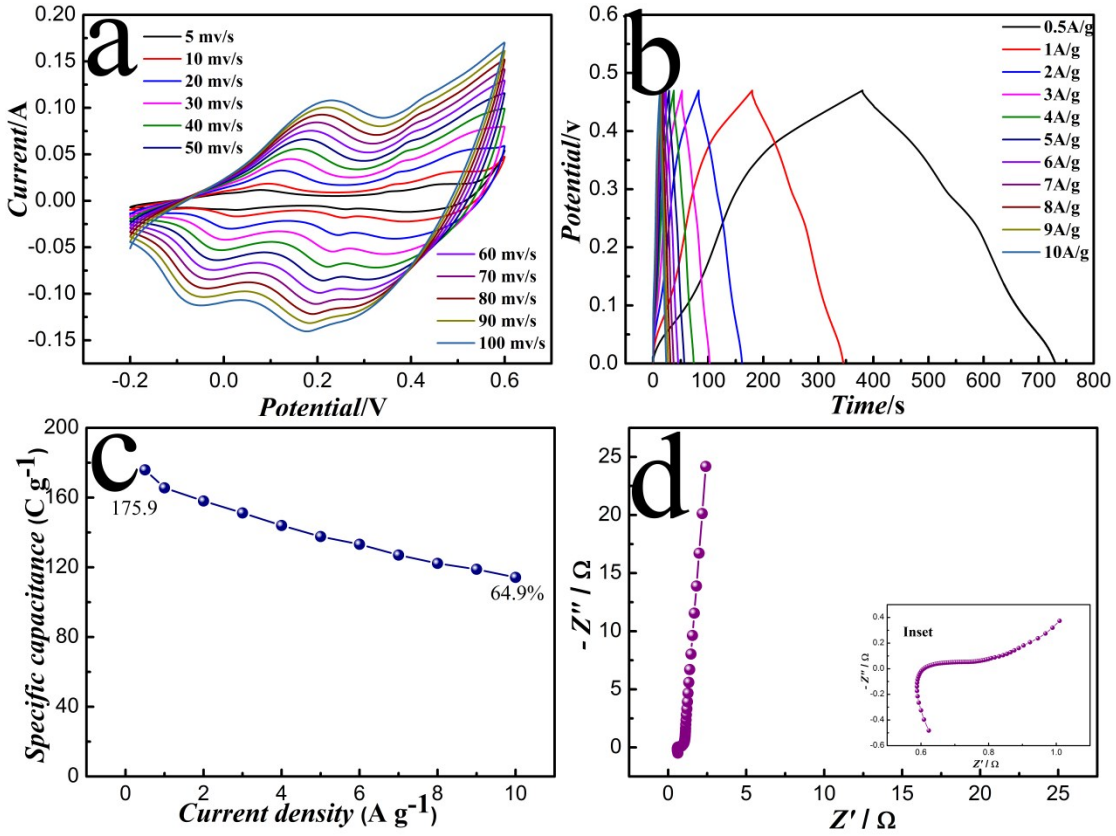

Figure S5. Three-electrode electrochemical measurements of the CoB-AC-2(C2) electrode.

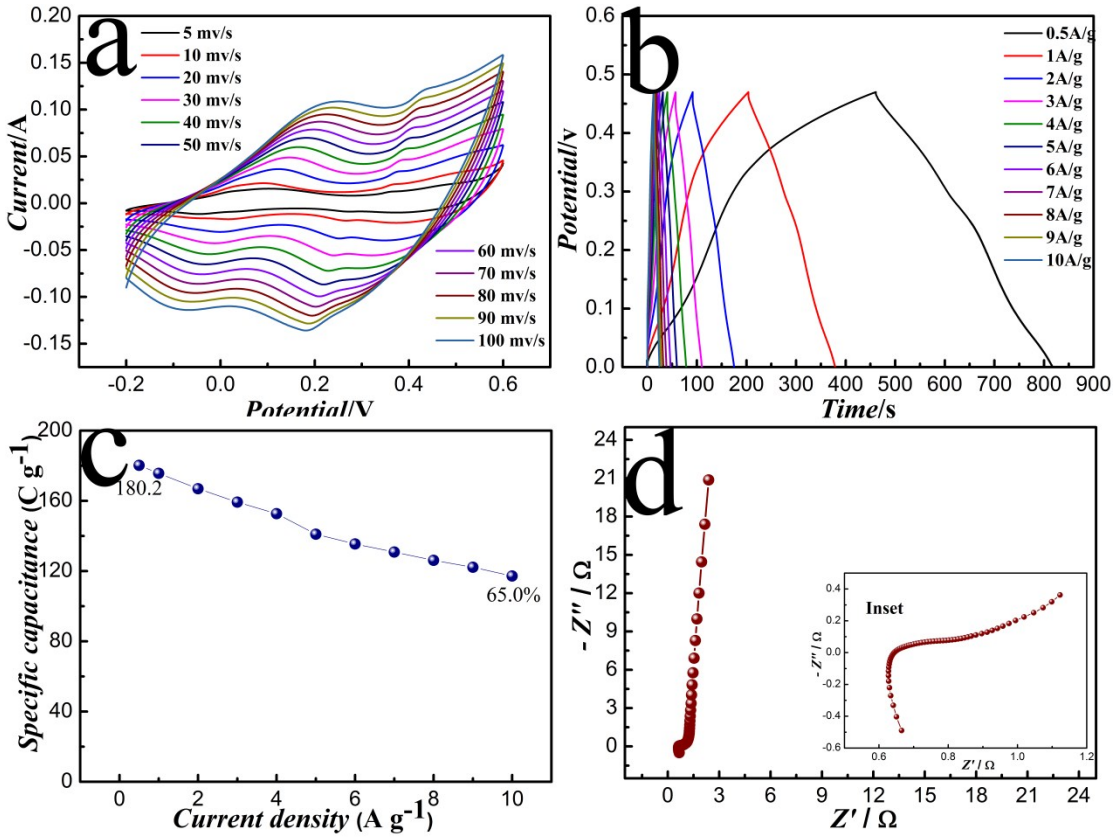

Figure S6. Three-electrode electrochemical measurements of the CoB-AC-4(C4) electrode.

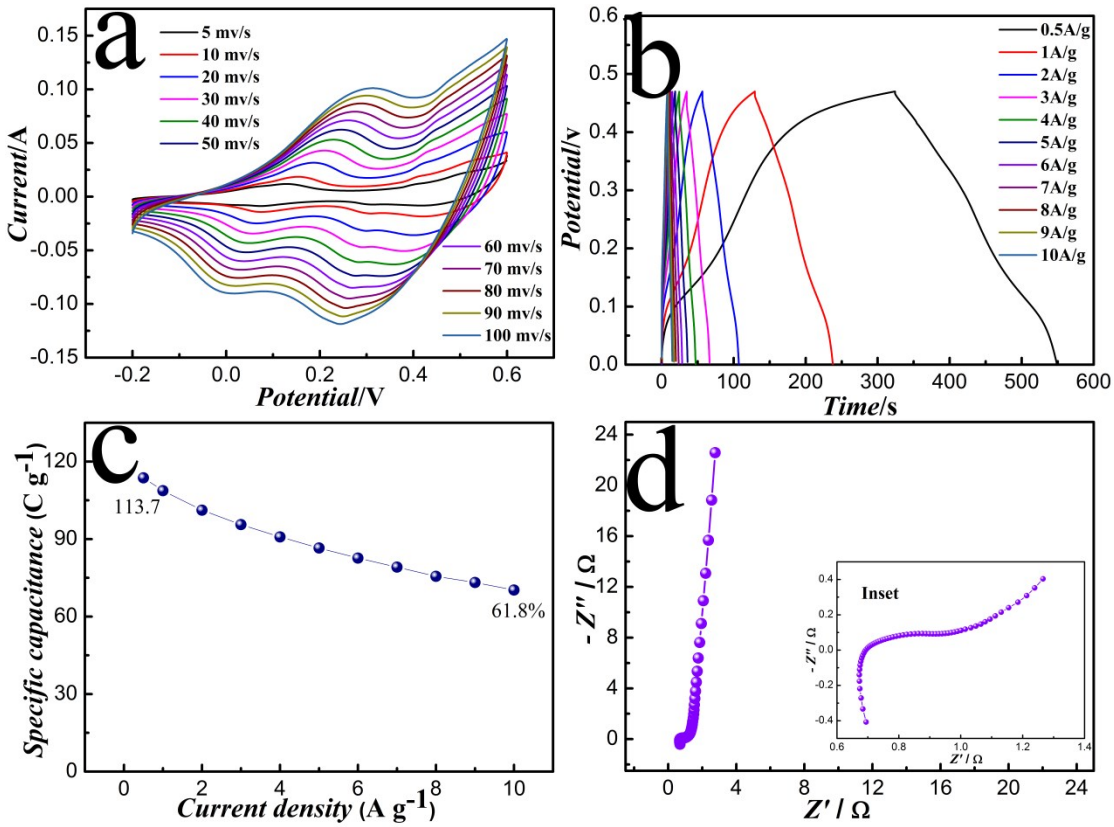

Figure S7. Three-electrode electrochemical measurements of the CoB-AC-5(C5) electrode.

Figure S3-7 show the electrochemical measurements of different CoB-AC electrodes. The cyclic voltammogram of CoB-containing samples exhibit undoubtedly the reversible faradaic redox reactions attributing to CoB. The platforms of the triangular shape shown by the galvanostatic charge-discharge curves correspond to the redox peaks of cyclic voltammogram. The specific capacitance of these electrodes increases first and then decreases. A small semi-circle is observed in the high-frequency range of the Nyquist plot, followed by a nearly vertical line in the lower frequency region. These results indicate a small charge transfer resistance and good capacitive behavior due to fast electron transport in the electrode/electrolyte interface and between the active electrode material and current collector.

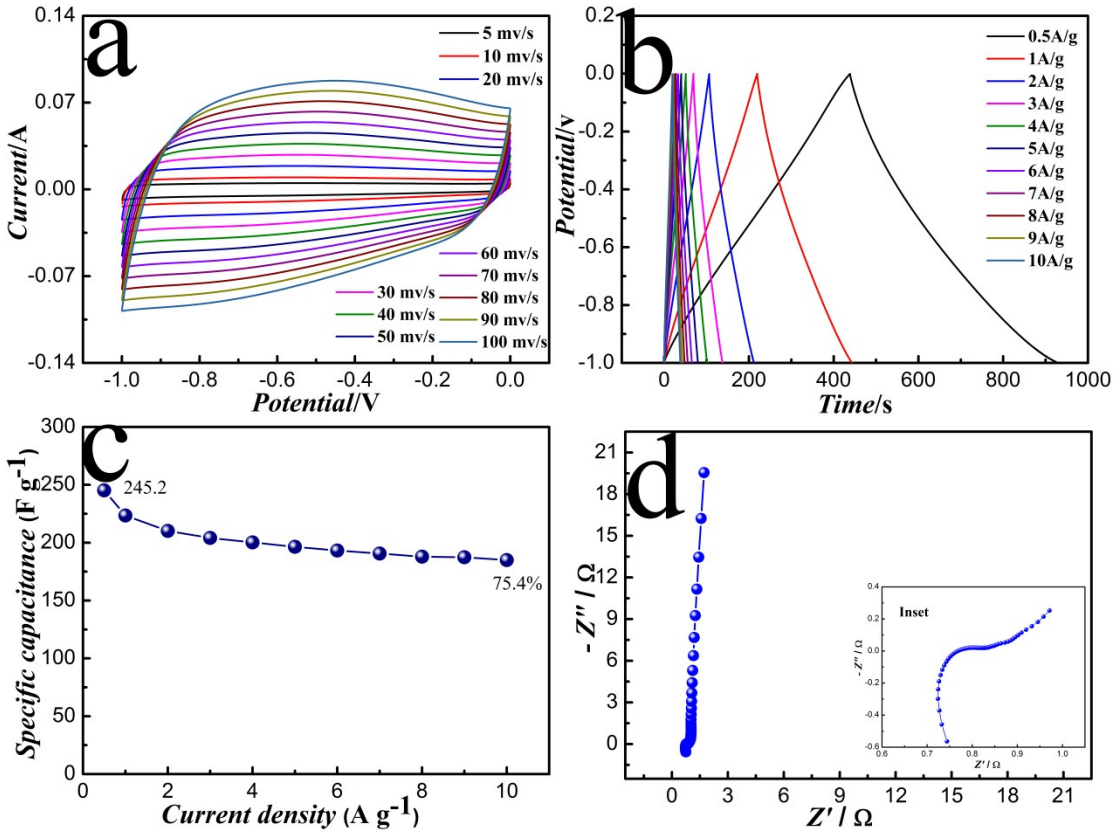

Figure S8 Three-electrode electrochemical measurements of the AC electrode. **a.** cyclic voltammograms of AC at variable scan rates from 5 to 100 mV s^{-1} within the potential window from -1.0 to 0.0 V. **b** galvanostatic charge-discharge curves at various current densities from 0.5 to 10 A g^{-1} within the potential window from -1.0 to 0 V; **c** specific capacitance as a function of the current densities and capacitance retention rate at various current densities; **d** Nyquist plots measured with an amplitude of 10 mV over the frequency range from 100 000 to 0.1 Hz, inset: the magnified high frequency region.

The CV test of AC is carried out in aqueous electrolytes(6 M KOH). It can be observed from **Figure S8a** that the CV curves of AC show excellent rectangular shapes from -1.0 to 0.0 V over a wide ranges of voltage scan rates, indicating an ideal electrical double layer effect of the tested supercapacitors, the fast electron transfer, and electrolyte ions diffusion. There is a clear contrast with the CV curves of the previous CoB-AC. More accurate GCD tests were conducted at different current densities, as shown in **Figure S8b**, where the GCD curves are not isosceles triangle due to the coexistence of EDLC and pseudocapacitance[5].

From the GCD curves, a decent specific capacitance(245.2 F g^{-1}) was calculated at a current density of 0.5 A g^{-1}. Note that the calculated specific capacitance of AC(**Figure S8c**) displays a decreasing tendency with the increase of GCD current density from 0.5 to 10 A g^{-1}. But at a current density of 10 A g^{-1} still owns a high specific capacitance of 185 F g^{-1}. The retention ratio was calculated to be 75.4% in the range of 1–20 A g^{-1}. The good rate performance reflects that the electrolyte ions could transfer rapidly and smoothly in the pores of this carbon. The Nyquist plot exhibits two distinct regions including a semicircle in the high-frequency region and a sloped line in the low-frequency region(**Figure S8d**). The nearly vertical line of all samples in the low-frequency region validates the conclusion that the dominant charge-storage mechanism for AC is EDLC. In the high-frequency region, the semicircle corresponds to the charge-transfer resistance at the electrode/electrolyte interface. Obviously, AC presents a small charge-transfer resistance, which is consequently related to its high electrical conductivity derived from its relatively high carbonization degree and moderate heteroatom doping level.

1. J. Zhao, H. Ma and J. Chen, *International Journal of Hydrogen Energy*, 2007, **32**, 4711-4716.
2. B. Guan, L. S. Fan, X. Wu, P. X. Wang, Y. Qiu, M. X. Wang, Z. K. Guo, N. Q. Zhang and K. N. Sun, *J Mater Chem A*, 2018, **6**, 24045-24049.
3. M. C. Liu, L. B. Kong, L. Kang, X. H. Li, F. C. Walsh, M. Xing, C. Lu, X. J. Ma and Y. C. Luo, *J Mater Chem A*, 2014, **2**, 4919-4926.
4. J. F. Gao, W. B. Zhang, Z. Y. Zhao and L. B. Kong, *Sustain Energ Fuels*, 2018, **2**, 1178-1188.
5. M. Gao, J. W. Fu, M. H. Wang, K. Wang, S. M. Wang, Z. W. Wang, Z. M. Chen and Q. Xu, *J Colloid Interf Sci*, 2018, **524**, 165-176.